Phys Chem Minerals (2006) 33: 417–425
DOI 10.1007/s00269-006-0089-7

ORIGINAL PAPER

Fabrizio Nestola · Tiziana Boffa Ballaran
Christian Liebske · Marco Bruno · Mario Tribaudino

High-pressure behaviour along the jadeite $NaAlSi_2O_6$–aegirine $NaFeSi_2O_6$ solid solution up to 10 GPa

Received: 14 December 2005 / Accepted: 14 April 2006 / Published online: 10 June 2006

Abstract The volume variation as a function of pressure along the jadeite–aegirine solid solution was determined at room temperature up to pressures between 6.5 and 9.7 GPa by single-crystal X-ray diffraction. The unit-cell volumes collected at room pressure for the different compositions indicate a slight deviation from linearity along the join. The pressure–volume data have been fitted using a third-order Birch-Murnaghan equation of state (BM3-EoS). The bulk modulus, K_{T0}, varies from 134.0(7) GPa for pure jadeite to 116.1(5) GPa for pure aegirine. Its evolution with composition along the join is not linear and can be described by the following second order polynomial:

$$K_{T0} = 116.2(5) + [0.25(3) \times (\text{mol\%Jd})] - [0.0008(3) \times (\text{mol\%Jd})^2] \quad (1)$$

The value of the first pressure derivative K' is close to 4 for all the samples investigated and can be used in a BM3-EoS to determine the volume variations of these pyroxenes up to 7–10 GPa. Along the join the highest compressibility among the crystallographic directions is always observed along **a**, however, the compression along **b** is the most affected by compositional changes. The strain ellipsoid analysis indicates that the major compression occurs on the (0 1 0) plane along **a** direction at about 145° to the **c** axis (from **c** to **a**). The anisotropy of the compression increases with increasing the aegirine component, as confirmed by the analysis of both the axial compressibility and the strain tensor.

Keywords High-pressure · Na-pyroxenes · Single-crystal · X-ray diffraction · Compressibility

F. Nestola (✉) · T. Boffa Ballaran · C. Liebske
Bayerisches Geoinstitut, Universitaet Bayreuth,
Universitaetstrasse 30, 95447 Bayreuth, Germany
E-mail: fabrizio.nestola@unipd.it
Tel.: +49-049-8272009
Fax: +49-049-8272010

F. Nestola
Department of Geosciences, Virginia Tech,
Crystallography Laboratory, Blacksburg, VA 24061, USA

Present address: F. Nestola
Dipartimento di Mineralogia e Petrologia,
Università degli Studi di Padova,
Corso Garibaldi 37, I-35137 Padova, Italy

Present address: C. Liebske
Institute for Mineralogy and Petrology,
Swiss Federal Institute of Technology ETH Zuerich,
CH-8092 Zurich, Switzerland

M. Bruno
Dipartimento di Scienze Mineralogiche e Petrologiche,
Universita' di Torino, Via Valperga Caluso 35,
10125 Torino, Italy

M. Tribaudino
Dipartimento di Scienze della Terra, Universita' di Parma,
Parco Area delle Scienze 157/A, 43100 Parma, Italy

Introduction

Clinopyroxenes are among the most studied minerals from the Earth's crust and upper mantle. In particular, Na-clinopyroxenes are the most common pyroxenes in the high-pressure metamorphic rocks, as blueschist metamorphic terranes, eclogites alkali-rich igneous rocks (Ernst et al. 1970; Clark and Papike 1968; Bailey 1969). They were also found in the eclogites from Kokchetav massif, which are considered to be the highest-pressure metamorphic terrane for the presence of abundant diamonds and coesite (Sobolev and Shatsky 1990; Zhang et al. 1997; Okamoto et al. 2000; Katayama et al. 2000). Experimental investigations showed that Na-rich pyroxenes are stable throughout the temperature/pressure range of the subducting slabs in the upper mantle (Schmidt 1993; Green et al. 2000). Further investigations at extreme conditions of temperature and pressure show that jadeite ($NaAlSi_2O_6$) transforms to $NaAlSiO_4$ ($CaFe_2O_4$-type structure) plus stishovite above 24 GPa (Liu 1978; Irfiune et al. 1994; Yagi et al. 1994) and that it is stable up to more than 20 GPa and 1,600°C (Tutti et al. 2000).

Jadeite is also involved in one of the most studied geobarometers, for which albite ($NaAlSi_3O_8$) transforms to jadeite + quartz (Newton and Smith 1967; Bell and Roseboom 1969; Johannes et al. 1971; Hays and Bell 1973; Holland 1980; Liu and Bohlen 1995), with a *P-T* line that can be described by $P = 0.35 + 0.0265T(°C) \pm 0.50$ kbar (Holland 1980). Cation substitution, very often present in natural samples, can affect the jadeite stability field and, therefore, shift the pressure at which the breakdown of albite occurs. Different authors have calculated the effects of diopside ($CaMgSi_2O_6$) and aegirine components ($NaFeSi_2O_6$) on the above reaction (Newton and Smith 1967; Kushiro 1969; Popp and Gilbert 1972; Holland 1983; Gasparik 1985; Liu and Bohlen 1995) with several approximations due to the lack of experimentally determined thermodynamic data (e.g. thermal expansion and compressibility). Thus, measurements of thermo-elastic properties are necessary for better constraining all petrological reactions in which jadeitic pyroxenes are involved, from the low-pressure albite breakdown (2–3 GPa and 1,100–1,500 K) to the very high-pressure phase transition of jadeite to $NaAlSiO_4$ above 20 GPa. Cameron et al. (1973) has determined the thermal expansion for jadeite and aegirine; two investigations have been performed at high-pressure on pure jadeite (Kandelin and Weidner 1988; Zhao et al. 1997).

In the present work we have synthesised pyroxenes with four different compositions along the jadeite–aegirine solid solution and studied them by high-pressure single-crystal X-ray diffraction using a diamond anvil cell. The aim of the work is to obtain precise and accurate EoS parameters along the jadeite–aegirine join. This will give an internally consistent compressibility data set, reliable for use in thermodynamic calculations up to 8–10 GPa for the jadeite–aegirine solid solution.

Experimental

Sample synthesis and characterization

We have synthesised four compositions along the jadeite–aegirine join: $Jd_{100}Ae_0$, $Jd_{74}Ae_{26}$, $Jd_{35}Ae_{65}$ and Jd_0Ae_{100}. Starting materials were prepared as glass by mixing appropriate amounts of the following compounds: SiO_2 (Fluka 99.9%), Na_2SiO_3 (Fluka≥97%), Fe_2O_3 (Alfa 99.9%), γ-Al_2O_3 (Merck 99.9%). Mixtures were ground and melted in a Pt crucible at 1,200°C for 2 h and then quenched into water. The so obtained glasses were finely ground and melted a second time following the same procedure in order to enhance homogeneity. Optical examinations confirmed vitrification and the absence of quench crystals. Only in the case of pure jadeite a slight iridescence suggested the presence of small amounts of very small quench crystals, which however, were undetectable by optical microscopy. Syntheses at high-pressure (HP) and high-temperature (HT) have been carried out using a 1,200 tonnes multi-anvil press at Bayerisches Geoinstitut. Samples were synthesised between 1,300 and 1,400°C and 6 GPa for 5–8 h. Quenching from HT was reached within a few seconds, while the decompression time at room T was of about 10–15 h. To avoid reduction of Fe^{3+} during synthesis at HP/HT, the required oxygen fugacity was constrained by a Re/ReO_2 oxygen buffer. All the synthesis products contained single phases of pyroxene crystals with sizes between 80 and 250 μm. Only the $Jd_{35}Ae_{65}$ composition showed a very small percentage of glass.

Chemical analyses were performed on the same crystals used for the compressibility studies by electron microprobe analyses (EMPA). The analyses were carried out using a Cameca SX-50, with an acceleration voltage of 15 kV and beam current of 15 nA (focused electron beam of approximately 2 μm). Counting times were 20 on the peak and 10 s on the background for each element. Internal correction routines of the instrument were used for data reduction and evaluation of element concentrations. The following synthetic minerals and oxides were used as standards: Si, Mg: enstatite; Al: spinel; Ca: wollastonite; Fe: wüstite; Ti, Mn: $MnTiO_3$; Cr: Cr_2O_3; Na: albite; Re: metal. Elements other than Na, Al and Fe, were also analysed in order to exclude the presence of impurities from the synthesis setup. Up to 10 point analyses were measured for each crystal. The averaged results are reported in Table 1. Each sample presented a very high chemical homogeneity.

Crystal-structure data were measured for all samples at ambient conditions and they will be published in a further work (Nestola et al. in preparation). Starting from the chemical analyses, the crystal-structure refinements gave the following compositions: $Jd_{100}Ae_0$, $Jd_{74}Ae_{26}$, $Jd_{35}Ae_{65}$, and Jd_0Ae_{100}. These compositions, very close to those obtained by microprobe analyses, were obtained following the same procedures used in several works performed on the cationic partitioning of Na-clinopyroxenes by crystal-structure refinement (Rossi et al. 1983; Oberti and Caporuscio 1991; Boffa Ballaran et al. 1998).

Table 1 Electron microprobe analyses of the single-crystals used for the high-pressure study (% by weight)

	$Jd_{100}Ae_0$	$Jd_{74}Ae_{26}$	$Jd_{35}Ae_{65}$	Jd_0Ae_{100}
SiO_2	59.87 (85)	57.04 (76)	54.34 (67)	52.10 (59)
Al_2O_3	25.63 (52)	18.18 (38)	8.49 (72)	-
[a]Fe_2O_3	-	8.88 (49)	21.04 (87)	34.03 (88)
Na_2O	15.58 (15)	14.96 (13)	14.09 (10)	13.50 (18)
Total	101.08	99.13	98.08	99.63
Cations per 6 oxygens				
Si	1.99 (1)	2.00 (1)	2.02 (1)	2.01 (1)
Al	1.00 (1)	0.75 (1)	0.37 (3)	-
Fe^{3+}	-	0.23 (1)	0.59 (3)	0.99 (1)
Na	1.00 (1)	1.02 (1)	1.02 (1)	1.01 (1)
[b]Total	3.99	4.00	4.00	4.01
No. analyses	7	6	10	8

[a]Total iron determined as FeO and recalculated as Fe_2O_3
[b]The sum of Ca, K, Mg, Ti, Mn, Cr, and Re never exceeded 0.004 atoms p.f.u. for all samples

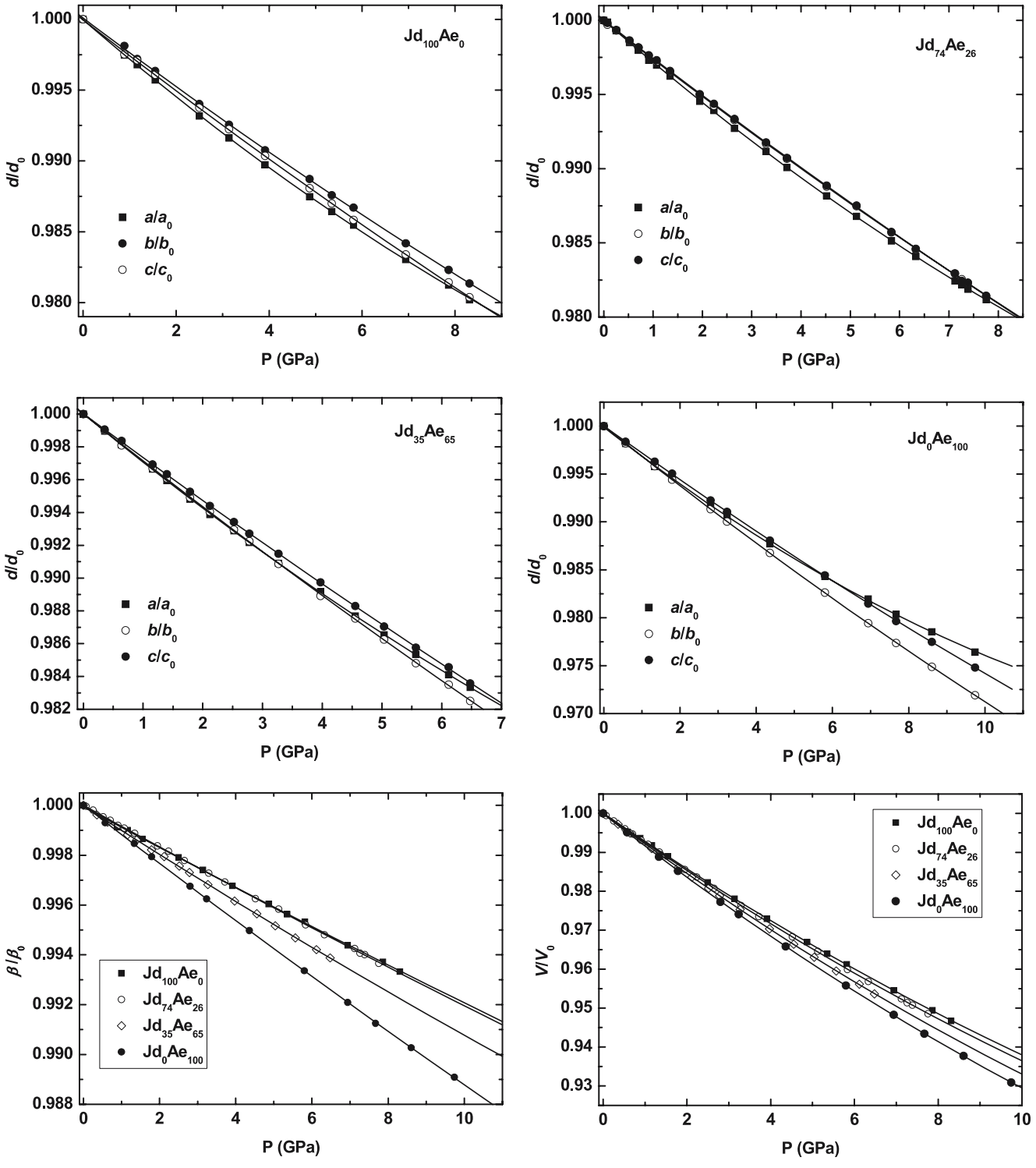

Fig. 1 Evolution of the unit-cell parameters and unit-cell volumes as a function of pressure for all the samples investigated. The symbols used are larger than the errors

High-pressure single-crystal X-ray diffraction

Single-crystals for the high-pressure X-ray measurements have been selected on the basis of their sharp extinction, crystal size, lack of twinning and sharp diffraction profile. The samples chosen had the following crystal sizes: $Jd_{100}Ae_0$: 140×48×35 μm^3; $Jd_{74}Ae_{26}$: 140×95×50 μm^3; $Jd_{35}Ae_{65}$: 140×70×55 μm^3; Jd_0Ae_{100}: 180×90×55 μm^3. The high-pressure diffraction experiments were performed with BGI design diamond-anvil cells (BGI-DAC), using steel gaskets (T301) pre-indented to a thickness ranging between 120 and 80 μm

Table 2 Pressures and unit-cell parameters for all the samples studied. One standard deviation is reported in parenthesis

P (Gpa)	*a*(Å)	*b*(Å)	*c*(Å)	*β*(°)	*V*(Å^3)
$Jd_{100}Ae_0$					
0.00010(1)	9.4278(3)	8.5651(4)	5.2262(2)	107.624(2)	402.21(2)
0.889(4)	9.4040(2)	8.5490(3)	5.2133(1)	107.530(2)	399.66(1)
1.163(12)	9.3976(3)	8.5412(3)	5.2111(3)	107.516(3)	398.89(2)
1.550(4)	9.3874(6)	8.5338(4)	5.2058(1)	107.479(3)	397.78(2)
2.499(5)	9.3634(3)	8.5139(2)	5.1936(2)	107.399(2)	395.08(2)
3.140(5)	9.3488(2)	8.5013(2)	5.1856(1)	107.345(2)	393.39(1)
3.914(6)	9.3309(2)	8.4859(2)	5.1758(1)	107.276(2)	391.33(2)
[a]4.870(8)	9.3097(5)	8.4685(7)	5.1639(3)	107.198(5)	388.92(4)
5.347(7)	9.2998(3)	8.4588(3)	5.1582(2)	107.154(3)	387.72(2)
[a]5.817(8)	9.2907(3)	8.4512(4)	5.1522(2)	107.121(3)	386.61(2)
6.939(6)	9.2679(3)	8.4296(4)	5.1394(2)	107.020(3)	383.93(2)
7.863(7)	9.2508(4)	8.4135(4)	5.1291(2)	106.948(3)	381.87(3)
8.309(9)	9.2411(4)	8.4053(5)	5.1236(3)	106.906(4)	380.78(3)
$Jd_{74}Ae_{26}$					
0.00010(1)	9.4781(2)	8.6180(3)	5.2449(2)	107.570(2)	408.43(2)
0.075(5)	9.4769(2)	8.6154(2)	5.2440(2)	107.566(2)	408.20(2)
0.255(4)	9.4715(2)	8.6121(2)	5.2415(2)	107.549(2)	407.65(2)
0.520(4)	9.4639(2)	8.6060(2)	5.2378(1)	107.521(2)	406.81(2)
0.706(4)	9.4590(2)	8.6022(2)	5.2353(1)	107.506(2)	406.26(2)
0.911(5)	9.4526(4)	8.5975(4)	5.2326(3)	107.484(4)	405.60(4)
1.074(4)	9.4495(2)	8.5940(2)	5.2308(2)	107.472(2)	405.19(2)
1.344(5)	9.4425(2)	8.5882(2)	5.2270(1)	107.450(2)	404.37(2)
1.949(4)	9.4264(3)	8.5748(3)	5.2188(2)	107.395(3)	402.54(2)
2.234(5)	9.4204(3)	8.5684(3)	5.2154(2)	107.372(3)	401.76(2)
2.652(5)	9.4091(2)	8.5600(2)	5.2100(1)	107.332(2)	400.57(2)
3.291(5)	9.3943(3)	8.5463(3)	5.2017(2)	107.277(3)	398.78(2)
3.717(6)	9.3840(3)	8.5376(3)	5.1963(2)	107.239(3)	397.61(2)
4.519(6)	9.3660(2)	8.5214(3)	5.1865(2)	107.167(2)	395.50(2)
5.126(6)	9.3528(3)	8.5100(3)	5.1794(2)	107.122(3)	393.97(3)
5.835(7)	9.3371(2)	8.4947(2)	5.1701(1)	107.054(2)	392.04(2)
6.330(8)	9.3272(3)	8.4848(3)	5.1641(2)	107.011(3)	390.80(2)
7.123(7)	9.3116(3)	8.4709(3)	5.1554(2)	106.952(3)	388.98(2)
[b]7.260(8)	9.3092(9)	8.4676(9)	5.1528(5)	106.932(8)	388.57(6)
7.386(7)	9.3064(3)	8.4654(3)	5.1521(2)	106.926(3)	388.31(2)
7.755(7)	9.2996(5)	8.4578(5)	5.1475(3)	106.888(5)	387.41(4)
$Jd_{35}Ae_{65}$					
0.00010(1)	9.5663(2)	8.7040(3)	5.2733(2)	107.600(2)	418.54(2)
0.358(3)	9.5564(2)	8.6954(3)	5.2684(2)	107.559(2)	417.39(2)
0.641(4)	9.5485(2)	8.6874(4)	5.2647(2)	107.528(2)	416.44(2)
1.160(3)	9.5342(2)	8.6752(3)	5.2571(2)	107.473(2)	414.76(2)
1.401(4)	9.5275(3)	8.6699(4)	5.2540(2)	107.450(3)	414.02(2)
1.788(3)	9.5167(2)	8.6597(4)	5.2483(2)	107.408(2)	412.72(2)
2.118(5)	9.5077(2)	8.6522(3)	5.2438(1)	107.379(2)	411.68(2)
2.521(4)	9.4982(2)	8.6426(4)	5.2386(2)	107.338(2)	410.50(2)
2.781(5)	9.4915(2)	8.6365(3)	5.2349(2)	107.310(2)	409.69(2)
3.269(4)	9.4793(2)	8.6245(3)	5.2284(2)	107.258(2)	408.21(2)
3.971(5)	9.4627(2)	8.6075(4)	5.2192(2)	107.187(3)	406.13(2)
4.553(5)	9.4485(2)	8.5955(4)	5.2116(2)	107.132(2)	404.48(2)
5.037(5)	9.4374(3)	8.5843(4)	5.2050(2)	107.080(3)	403.07(3)
5.567(5)	9.4261(2)	8.5718(4)	5.1982(2)	107.028(3)	401.60(2)
6.119(6)	9.4142(2)	8.5604(4)	5.1919(3)	106.977(3)	400.18(3)
[c]6.476(6)	9.4068(3)	8.5517(4)	5.1867(2)	106.941(3)	399.14(3)
Jd_0Ae_{100}					
0.00010(1)	9.6623(4)	8.8000(2)	5.2956(4)	107.579(3)	429.25(3)
0.574(4)	9.6446(4)	8.7841(3)	5.2870(4)	107.504(4)	427.17(4)
1.335(5)	9.6216(3)	8.7633(2)	5.2759(3)	107.414(3)	424.46(2)
1.791(4)	9.6092(4)	8.7508(2)	5.2693(5)	107.357(4)	422.91(4)
2.804(4)	9.5817(4)	8.7237(2)	5.2545(4)	107.230(3)	419.50(3)
3.237(5)	9.5715(5)	8.7123(2)	5.2482(4)	107.175(4)	418.13(4)
4.360(5)	9.5435(3)	8.6835(2)	5.2324(3)	107.038(3)	414.58(3)
5.799(6)	9.5107(3)	8.6471(2)	5.2131(3)	106.865(3)	410.28(3)
6.940(7)	9.4879(4)	8.6190(2)	5.1975(3)	106.728(3)	407.04(3)
7.668(7)	9.4726(3)	8.6008(2)	5.1878(3)	106.638(3)	404.96(2)

Table 2 (Contd.)

P (Gpa)	a(Å)	b(Å)	c(Å)	β(°)	V(Å^3)
8.607(7)	9.4549(3)	8.5789(2)	5.1763(3)	106.533(3)	402.51(2)
[c]9.741(9)	9.4344(4)	8.5529(2)	5.1622(4)	106.405(4)	399.58(3)

[a]Data measured during decompression
[b]This datum measured during decompression presents a slight broadening of the Bragg reflections
[c]The crystal was broken during a further increase of pressure and the experiments were therefore interrupted

and holes with diameters between 350 and 250 μm. Single-crystals of quartz were used as internal diffraction pressure standards (Angel et al. 1997) and a mixture of methanol: ethanol: water with ratios of 16:3:1 was used as hydrostatic pressure medium. Unit-cell parameters were determined at each pressure using a four-circle Huber diffractometer operating at 50 kV and 40 mA by centring 20–22 Bragg reflections between 10° and 32° in 2θ. Typical half-widths of the reflections were between 0.080° and 0.130° in ω. Angel et al. (2000) provided full details of the instrument used and the peak centring algorithms. During the centring procedure the effects of crystal offsets and diffractometer aberrations were eliminated from refined peak positions by the eight-position centring method of King and Finger (1979). Unconstrained unit-cell parameters, obtained by vector least-squares (Ralph and Finger 1982), were found to be within one estimated standard deviation with respect to the symmetry-constrained ones. All the unit-cell parameter data at different pressures are reported in Table 2.

Results

Equation of state and compressibility

The unit-cell data collected at room pressure for pure end-members jadeite and aegirine are in good agreement with previous published data (Prewitt and Burnham 1966; Cameron et al. 1973; Zhao et al. 1997; Redhammer et al. 2000). The evolutions of the unit-cell parameters as a function of pressure for all samples studied are reported in Fig. 1. They show a continuous behaviour with pressure and no evidence for phase transitions was found in the investigated pressure range. The unit-cell parameters b, c and the β angles vary almost linearly with pressure, whereas the unit-cell parameters a show a strong non-linearity. The pressure-volume (P-V) data of all the samples have been fitted using a third-order Birch-Murnaghan equation of state, refining simultaneously the unit-cell volume at room pressure V_0, the bulk modulus K_{T0} and its first pressure derivative K' using the EOSFIT 5.2 program (Angel 2002). The BM3-EoS refined coefficients are reported in Table 3. The f_E-F_E plots with F_E normalized stress defined as $F_E = P/3f_E(1+2f_E)^{5/2}$ and the finite strain f_E defined as $f_E = [(V_0/V)^{2/3}-1]/2$ (Angel 2000) are reported in Fig. 2. Such plots can be used for the correct choice of the equation of state to be used for fitting the P-V data and give an indication of the quality of the experimental data. By the f_E-F_E plots of Fig. 2 it appears that all our data lie on practically horizontal lines indicating that a BM-EoS truncated at the second order (i.e. K' fixed to the value of four) would be sufficient to describe the evolution with pressure of the volumes of these clinopyroxenes. However, given the accuracy of our data we decided to use a BM3-EoS for the fitting procedure, refining thus K' and obtaining values very close to four (Table 3).

The values of K_{T0} obtained using the BM3-EoS are plotted vs composition in Fig. 3. K_{T0} increases with increasing jadeitic component and has a small positive

Table 3 Eos coefficients resulting from the fits using a BM3-EoS for volumes and unit-cell parameters. The relative compressibility data ($\beta = -1/3K_0$ for unit-cell parameters and $-1/K_0$ for unit-cell volumes) are also reported

	$Jd_{100}Ae_0$	$Jd_{74}Ae_{26}$	$Jd_{35}Ae_{65}$	Jd_0Ae_{100}
a_0 (Å)	9.4279(3)	9.4785(2)	9.5666(2)	9.6625(3)
K_{a0} (GPa)	113.9(8)	112.4(7)	108.8(7)	99.8(7)
K'	6.7(2)	6.5(2)	6.4(3)	8.9(2)
β_{a0} (GPa^{-1})	−0.00293(2)	−0.00296(2)	−0.00306(2)	−0.00334(2)
b_0 (Å)	8.5665(6)	8.6177(2)	8.7041(2)	8.8001(2)
K_{b0} (GPa)	131.4(2.3)	127.7(8)	115.3(9)	104.2(3)
K'	3.7(6)	2.9(2)	2.3(3)	2.2(1)
β_{b0} (GPa^{-1})	−0.00254(4)	−0.00261(2)	−0.00289(2)	−0.00320(1)
c_0 (Å)	5.2262(2)	5.2449(1)	5.2735(1)	5.2958(3)
K_{c0} (GPa)	129.0(3.6)	128.9(7)	123.3(9)	115.5(1.2)
K'	2.8(1.2)	2.5(2)	2.3(3)	2.5(3)
β_{c0} (GPa^{-1})	−0.00258(7)	−0.00258(1)	−0.00270(2)	−0.00289(3)
V_0 (Å^3)	402.26(2)	408.44(1)	418.57(2)	429.26(2)
K_0 (GPa)	134.0(7)	130.4(5)	124.4(6)	116.1(5)
K'	4.4(1)	4.5(2)	3.9(2)	4.4(1)
β_{V0} (GPa^{-1})	−0.00746(5)	−0.00767(3)	−0.00804(4)	−0.00861(4)

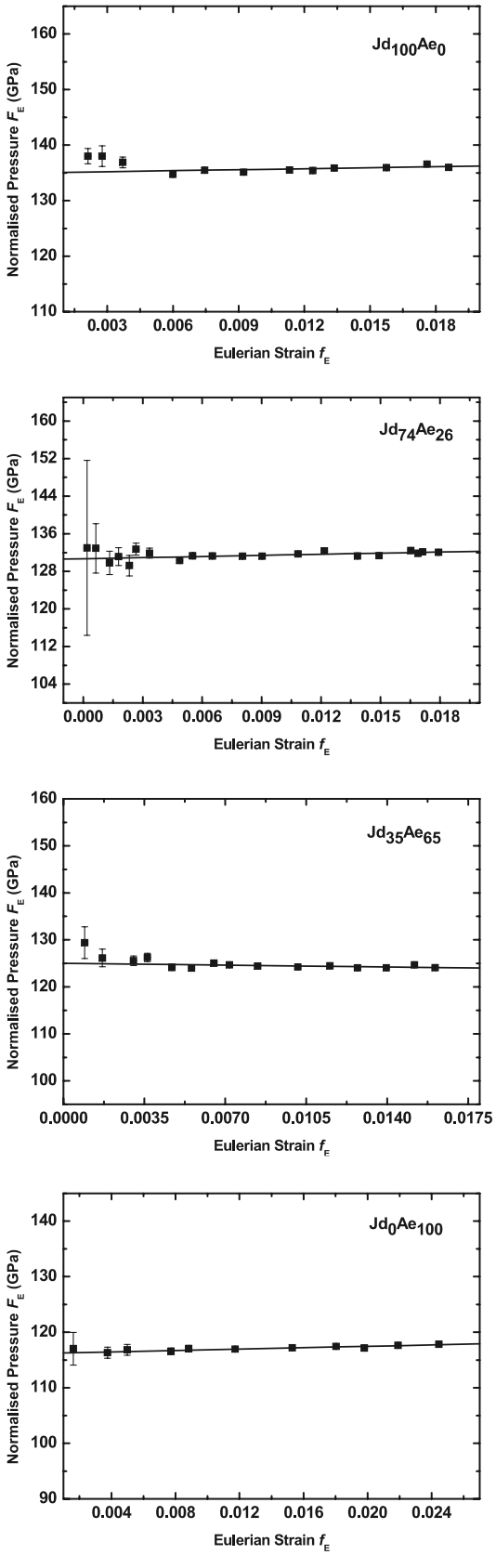

Fig. 2 The f_E-F_E plots for all the compositions. The normalised stress F_E is defined as $F_E = P/3f_E(1 + 2f_E)^{5/2}$, while the finite strain f_E is defined as $f_E = [(V_0/V)^{2/3} - 1]/2$

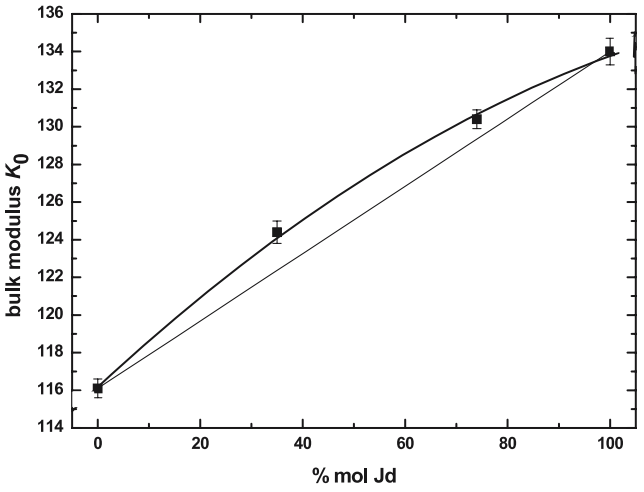

Fig. 3 Evolution of the bulk modulus K_{T0} with composition. The values of K_{T0} are from Table 3, while those of compositions from Table 1 transformed in % molar of jadeite. The error estimated for the compositions is of about 1% molar

deviation from linearity, which appears symmetric. The K_{T0} vs composition trend can be described by:

$$K_{T0} = 116.2(5) + [0.25(3) \times (\text{mol\%Jd})] - [0.0008(3) \times (\text{mol\%Jd})^2] \quad (1)$$

A BM3-EoS was also used for fitting the evolutions with pressure of the unit-cell parameters a, b and c (Table 3).

The values of compressibility β_0, calculated as $\beta_0 = -1/3\ K_{T0}$ for unit-cell parameters and $-1/K_{T0}$ for unit-cell volumes, are also reported in Table 3. The compressibility scheme is $\beta_{a0} > \beta_{b0} \cong \beta_{c0}$ for $Jd_{100}Ae_0$ and $Jd_{74}Ae_{26}$. The compressional anisotropy increases for $Jd_{35}Ae_{65}$ and Jd_0Ae_{100} for which $\beta_{a0} > \beta_{b0} > \beta_{c0}$. Among the crystallographic axes the **a** direction is always that of maximum deformation for our Na-clinopyroxenes. However, an analysis of the strain tensor (STRAIN

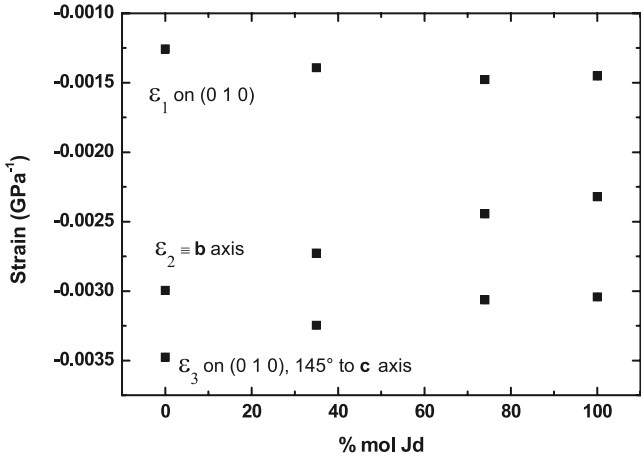

Fig. 4 Evolution of the strain ellipsoid axes with pressure for all samples here studied (STRAIN, Ohashi 1982). The symbols used are larger than the errors

Table 4 Strain ellipsoid axes and their orientation for all the compositions here studied. The calculation was performed using the STRAIN program (Ohashi 1982). The angle between ε_3 and **c** is measured from **c** to **a** as in Finger and Ohashi (1976)

	Unit strain (GPa^{-1})			
	ε_1	ε_2	ε_3	$\hat{\varepsilon_3}$ c (°)
$Jd_{100}Ae_0$	−0.00145(1)	−0.00232(1)	−0.00304(1)	145.9(2)
$Jd_{74}Ae_{26}$	−0.00148(1)	−0.00244(1)	−0.00306(1)	146.6(2)
$Jd_{35}Ae_{65}$	−0.00139(1)	−0.00273(1)	−0.00325(1)	145.2(2)
Jd_0Ae_{100}	−0.00126(1)	−0.00300(1)	−0.00348(1)	144.2(2)

program, Ohashi 1982) is useful for determining the major deformation directions. In monoclinic pyroxenes physically the strain tensor corresponds to an ellipsoid with an axis coincident with the **b** axis, and the others two lying onto the (010) plane (Ohashi and Burnham 1973). The strain ellipsoid was calculated in the examined samples by comparing the unit-cell parameters at room pressure with those measured at P between 5.1 and 5.8 GPa for the different samples, in order to obtain homogeneous ranges (Fig. 4). The more deformed axis was on the (0 1 0) plane, at about 145° to the **c** axis, measured from c to a as in Finger and Ohashi (1976). The orientation of the strain ellipsoid does not change with composition, however, as observed for the axial compressibility, the anisotropy of the strain axes increases with increasing the aegirine component along the solid solution (Table 4). For jadeite the axial ratios of the strain ellipsoid are 1.00:1.60:2.10, whereas they are 1.00:2.38:2.76 for pure aegirine.

Discussion

As a main result it was observed that along the solid solution jadeite–aegirine the bulk modulus K_{T0} decreases from 134.0 GPa for pure jadeite down to 116.1 GPa for pure aegirine. This decrease is non-linear and it can be described as a function of composition by Eq. 1. Moreover, the first pressure derivative of bulk modulus, K', remains practically constant along the join with a value very close to four. Our results clearly show that for Na-clinopyroxenes the bulk modulus is mainly controlled by the size of the M1 structural site, whereas the value of K' appears to be controlled by that of the M2 site. Such observations are confirmed by the unpublished data collected at high-pressure along the join $NaCrSi_2O_6$–$CaMgSi_2O_6$ (Boffa Ballaran et al. in preparation) and by further unpublished data always collected at high-pressure along the jadeite–hedenbergite join ($CaFeSi_2O_6$) (Nestola et al. in preparation); both such works were performed using the same experimental procedures of the present study. In Thompson et al. (2005) BM3-EoS coefficients for aegirine of $K_{T0} = 125.1(4.5)$ and $K' = 1.9(7)$ are reported; they are in very bad agreement with our aegirine coefficients. However, we agree with the model of

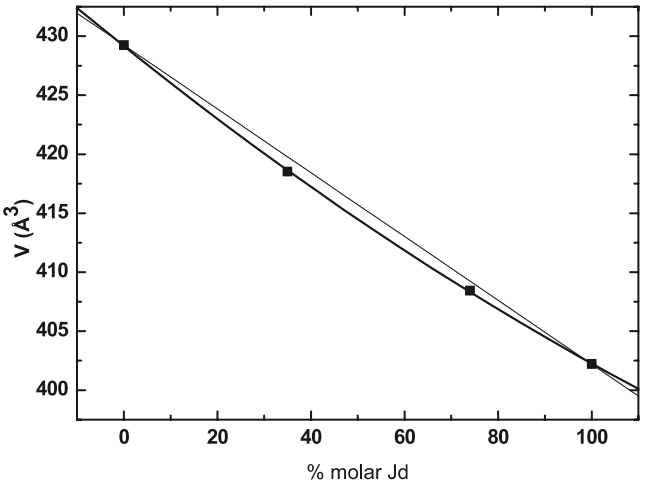

Fig. 5 Evolution of the unit-cell volumes V_0 with composition. The values of V_0 and those of compositions are from Table 2 and transformed in % molar of jadeite. The error estimated for the compositions is of about 1% molar. The symbols used are larger than the errors

Thompson et al. (2005) and Thompson and Downs (2004) who propose that for $C2/c$ clinopyroxenes is the M1 site that controls their compressibility as confirmed also in Bindi et al. (in press) for a K-rich $C2/c$ clinopyroxene.

The analysis of the strain tensor of our data indicates that the compressional anisotropy increases with increasing aegirine content along the solid solution (Fig. 4). Therefore, with increasing cationic radius at the M1 site the anisotropy increases. A similar behaviour is shown by diopside and hedenbergite ($CaMgSi_2O_6$ and $CaFeSi_2O_6$, respectively, Zhang et al. 1997), with hedenbergite showing much higher anisotropy than diopside. In our opinion these differences in anisotropy are not related to the size of the M1 cation only. In fact, based on Shannon (1976), although the difference in cationic radius between Al (in jadeite) and Fe^{3+} (in aegirine) is 0.11 Å, while between Mg (in diopside) and Fe^{2+} (in hedenbergite) is 0.06 Å, the difference in anisotropy between hedenbergite and diopside is much higher than that observed between jadeite and aegirine. Such observations could suggest that there could be some effect due to the 3d transition elements, as found in Nestola et al. (2005) on the compressibility of clinopyroxenes.

Our data give a further important result: the unit-cell volume at ambient conditions is non-linear with composition (Fig. 5). The deviation from linearity indicates that jadeite–aegirine solid solution is not a completely ideal mixing as reported by previous investigations (Newton and Smith 1967; Popp and Gilbert 1972; Liu and Bohlen 1995). In Fig. 5, however, we can note that the deviation from linearity is very small and the excess volumes are only 0.20% for $Jd_{74}Ae_{26}$ and 0.30% for $Jd_{35}Ae_{65}$. Even if such differences are very limited we consider them significant. For

this reason a determination of the excess volume at room pressure and higher pressure, by fitting the data with an asymmetrical solution model (Spear 1993) is in progress.

High-temperature in situ measurements are in progress in order to determine the room pressure thermal expansion of the same samples used in this work for the high-pressure investigation. This will provide a complete experimental thermodynamic data set for one of the most important mineral families in earth science.

Acknowledgments This project was supported by the Alexander von Humboldt Foundation to Fabrizio Nestola and was improved through discussions with Friedrich Seifert and Catherine McCammon. We thank Charles T. Prewitt and Richard M. Thompson for their helpful reviews. We wish to thank Detlef Krauße and Anke Potzel for collecting the electron microprobe data and Hubert Schulze for preparing thin sections from single-crystal for microprobe analyses.

References

Angel RJ (2000) Equations of State. In: Hazen RM, Downs RT (eds) High-temperature and high-pressure crystal chemistry. Reviews in Mineralogy and Geochemistry, vol. 41. Mineralogical Society of America and Geochemical Society, Washington, pp 35–39

Angel RJ (2002) EOSFIT V5 2 Crystallography Laboratory. Department of Geological Sciences Virginia Tech, USA

Angel RJ, Allan DR, Miletich R, Finger LW (1997) The use of quartz as an internal pressure standard in high pressure crystallography. J Appl Crystallogr 30:461–466

Angel RJ, Downs RT, Finger LW (2000) High-temperature and high-pressure diffractometry. In: Hazen RM, Downs RT (eds) High-temperature and high-pressure crystal chemistry. Reviews in Mineralogy and Geochemistry, vol. 41. Mineralogical Society of America and Geochemical Society, Washington, pp 559–596

Bailey DK (1969) The stability of acmite in the presence of H_2O. Am J Sci 267A:1–16

Bell PM, Roseboom EH (1969) Melting relations of jadeite and albite to 45 kilobars with comments on melting diagrams of binary systems at high pressures. Min Soc Am Mem 97:97–173

Boffa Ballaran T, Carpenter M, Domeneghetti MC, Tazzoli V (1998) Structural mechanisms of solid solution and cation ordering in augite-jadeite pyroxenes: I. A macroscopic perspective. Am Miner 83:419–433

Cameron M, Sueno S, Prewitt CT, Papike JJ (1973) High temperature crystal chemistry of acmite, diopside, hedenbergite, jadeite, spodumene, and ureyite. Am Miner 58:594–618

Clark JR, Papike JJ (1968) Crystal-chemical charcaterization of omphacites. Am Miner 53:840–868

Ernst WG, Seki Y, Onuki H, Gilbert MC (1970) Comparative study of low-grade metamorphism in the Californai Coast ranges and the outer metamorphic belt of Japan. Geol Soc Am Mem 124:276

Finger LW, Ohashy Y (1976) Thermal-expansion of diopside to 800°C and a refinement of crystal-structure at 700°C. Am Miner 61:303–310

Gasparik T (1985) Experimental determined compositions of diopside-jadeite pyroxene in equilibrium with albite and quartz at 1200–1350°C and 15–34 kbar. Geochim Cosmochim Acta 49:865–870

Green H, Dobrzhinetskaya L, Bozhilov K (2000) Mineralogical and experimental evidence for very deep exhumation from subduction zones. J Geodynam 30:61–76

Hays JF, Bell PM (1973) Albite-jadeite-quartz equilibrium: a hydrostatic determination. Carnegie Inst Washington Year b 72:706–708

Holland TJB (1980) The reaction albite = jadeite + quartz determined experimentally in the range 600–1200°C. Am Miner 65:129–134

Holland TJB (1983) The experimental determination of activities in disordered and short-range ordered jadeitic pyroxenes. Contrib Petrol Miner 82:214–220

Irfiune T, Ringwood AE, Hibberson WO (1994) Subduction continental crust and terrigenous and pelagic sediments: an experimental study. Earth Planet Sci Lett 126:351–368

Johannes W, Bell PM, Boettcher AL, Chipman DW, Hays JF, Mao HK, Newton RC, Seifert C (1971) An inter-laboratory comparison of piston-cylinder pressure calibration using albite-breakdown reaction. Contrib Miner Petrol 32:24–38

Kandelin J, Weidner DJ (1988) The single-crystal elastic properties of jadeite. Phys Earth Planet Int 50:251–260

Katayama I, Zayachkovsky AA, Maruyama S (2000) Prograde pressure–temperature records from inclusions in zircons from ultrahigh-pressure–high-pressure rocks of the Kokchetav Massif, northern Kazakhstan. Island Arc 9:417–427

King H, Finger LW (1979) Diffracted beam crystal centering and its application to high-pressure crystallography. J Appl Crystallogr 12:374–378

Kushiro I (1969) Clinopyroxene solid solution formed by reactions between diopside and plagioclase at high pressure. Miner Soc Am Spec Pap 2:179–191

Liu L (1978) High-pressure phase transformation of albite, jadeite and nepheline. Earth Planet Sci Lett 37:438–444

Liu J, Bohlen R (1995) Mixing properties and stability of jadeite-acmite pyroxene in the presence of albite and quartz. Contrib Miner Petrol 119:433–440

Nestola F, Boffa Ballaran T, Tribaudino M, Ohashi H (2005) Compressional behaviour of $CaNiSi_2O_6$: bulk modulus systematic and cation type in clinopyroxenes. Phys Chem Miner 32:222–227

Newton RC, Smith JV (1967) Investigations concerning the breakdown of albite in the earth. J Geol 75:268–286

Oberti R, Caporuscio FA (1991) Crystal chemistry of clinopyroxenes from mantle eclogites: a study of the key role of the M2 site population by means of crystal-structure refinement. Am Miner 76:1141–1152

Ohashi Y (1982) A program to calculate the strain tensor from two sets of unit-cell parameters. In: Hazen RM, Finger LW (eds) Comparative crystal chemistry. Wiley, Chechester, pp 92–102

Ohashi Y, Burnham CW (1973) Clinopyroxene lattice deformations: the roles of chemical substitution and temperature. Am Miner 58:843–849

Okamoto K, Liou JG, Ogasawara Y (2000) Petrology of the diamond-grade eclogite in the Kokchetav Massif, northern Kazakhstan. Island Arc 9:379–399

Popp RK, Gilbert MC (1972) Stability of acmite-jadeite pyroxenes at low pressure. Am Miner 51:1210–1231

Prewitt CT, Burnham CW (1966) The crystal structure of jadeite. Am Miner 51:956–975

Ralph RL, Finger LW (1982) A computer program for refinement crystal orientation matrix and lattice constants from diffractometer data with lattice symmetry constrains. J Appl Crystallogr 15:537–539

Redhammer GJ. Amthauer G, Lottermoser W, Treutmann W (2000) Synthesis and structural properties of clinopyroxenes of the hedenbergite $CaFe^{2+}Si_2O_6$–aegirine $NaFe^{3+}Si_2O_6$ solid-solution series. Eur J Miner 12:105–120

Rossi G, Smith DC, Ungaretti L, Domeneghetti MC (1983) Crystal-chemistry and cation ordering in the system diopside-jadeite: a detailed study by crystal structure refinement. Contrib Petrol Miner 83:247–258

Schmidt M (1993) Phase-relations and compositions in tonalites as a function of pressure—an experimental study at 650°C. Am J Sci 10:1011–1060

Shannon (1976) Revised effective ionic radii and systematic studies of interatomic distances in halides and chalcogenides. Acta Crystallogr A32:751

Sobolev NV, Shatsky VS (1990) Diamond inclusions in garnets from metamorphic rocks—a new environment for diamond formation. Nature 343:742–746

Spear FS (1993) Metamorphic phase equilibria and pressure–temperature–time paths. Mineralog Soc Am, Washington

Thompson RM, Downs RT, Redhammer GJ (2005) Model pyroxenes III: volume of $C2/c$ pyroxenes at mantle P, T and, x. Am Miner 90:1840–1851

Tutti F, Dubrovinsky L, Saxena SK (2000) High pressure phase transformation of jadeite and stability of $NaAlSiO_4$ with calcium-ferrite type structure in the lower mantle conditions. Geophys Res Lett 27:2025–2028

Yagi A, Suzki T, Akaogi M (1994) High-pressure transitions in the system $KAlSi_3O_8$–$NaAlSi_3O_8$. Phys Chem Miner 21:12–17

Zhang L, Ahsbahs H, Hafner SS, Kutoglu A (1997) Single-crystal compression and crystal structure of clinopyroxene up to 10 GPa. Am Miner 82:245–258

Zhao Y, Von Dreele RB, Shankland TJ, Weidner DJ, Zhang JZ, Wang YB, Gasparik T (1997) Thermoelastic equation of state of jadeite $NaAlSi_2O_6$: an energy-dispersive Reitveld refinement study of low symmetry and multiple phases diffraction. Geophys Res Lett 24:5–8